

This article was downloaded by:

On: 24 January 2011

Access details: *Access Details: Free Access*

Publisher *Taylor & Francis*

Informa Ltd Registered in England and Wales Registered Number: 1072954 Registered office: Mortimer House, 37-41 Mortimer Street, London W1T 3JH, UK



## Journal of Liquid Chromatography & Related Technologies

Publication details, including instructions for authors and subscription information:

<http://www.informaworld.com/smpp/title~content=t713597273>

### A Simple Method of Evaluating Particle Size Distributions and Settling Rates for Silica Based Chromatographic Supports

D. A. Hanggi<sup>a</sup>; P. W. Carr<sup>a</sup>

<sup>a</sup> Department of Chemistry Smith & Kolthoff Halls, University of Minnesota, Minneapolis, MN

**To cite this Article** Hanggi, D. A. and Carr, P. W.(1984) 'A Simple Method of Evaluating Particle Size Distributions and Settling Rates for Silica Based Chromatographic Supports', *Journal of Liquid Chromatography & Related Technologies*, 7: 12, 2323 – 2349

**To link to this Article:** DOI: 10.1080/01483918408068881

**URL:** <http://dx.doi.org/10.1080/01483918408068881>

PLEASE SCROLL DOWN FOR ARTICLE

Full terms and conditions of use: <http://www.informaworld.com/terms-and-conditions-of-access.pdf>

This article may be used for research, teaching and private study purposes. Any substantial or systematic reproduction, re-distribution, re-selling, loan or sub-licensing, systematic supply or distribution in any form to anyone is expressly forbidden.

The publisher does not give any warranty express or implied or make any representation that the contents will be complete or accurate or up to date. The accuracy of any instructions, formulae and drug doses should be independently verified with primary sources. The publisher shall not be liable for any loss, actions, claims, proceedings, demand or costs or damages whatsoever or howsoever caused arising directly or indirectly in connection with or arising out of the use of this material.

A SIMPLE METHOD OF EVALUATING PARTICLE SIZE  
DISTRIBUTIONS AND SETTLING RATES FOR SILICA  
BASED CHROMATOGRAPHIC SUPPORTS

D.A. Hanggi and P.W. Carr  
Department of Chemistry  
Smith & Kolthoff Halls  
University of Minnesota  
Minneapolis, MN 55455

ABSTRACT

A simple and inexpensive method of evaluating particle settling rates and the particle size distribution of chromatographic supports using common laboratory equipment is reported. The time dependence of the turbidity of a solution of silica support particles suspended in an appropriate liquid is measured on a spectrometer. Digital acquisition allows data manipulation using simple algorithms to yield the distribution of particle sizes based on the Stoke's diameter. This data can easily be transformed into the most useful form for presentation, e.g. number average, weight average, cumulative distribution, etc.

INTRODUCTION

Knowledge of the average particle size and the particle size distribution is useful in the evaluation of the efficiency of chromatographic columns. Measurement of the reduced plate height ( $h=H/d$ ) and velocity ( $v=ud/D$ ) require estimates of the particle size ( $d$ ). It is not clear what the best measure of particle size

should be, e.g. number average, cumulative weight average, etc. Differences in the values of the weight and number averages, however, often vary as much as 20% for small (3 and 5  $\mu\text{m}$ ) particles. In addition, because commercial packing materials are not perfectly monodisperse, a knowledge of the distribution is useful since column efficiency will tend to reflect the largest particles present while net pressure drops will be most influenced by the smallest particles [1]. In this context alternative efficiency calculations suggested by Bristow [2] and Halasz [3] which are based on the column pressure drop, permeability, or flow resistance parameter weight the smallest particles most heavily in the determination of an effective particle diameter.

The particle size and distribution will vary widely not only between different manufacturers and types of supports, but also between lots of the same silica. In addition, the manufacturer's provided particle size is often not measured directly for a particular lot, or the method of analysis is not stated. Because the actual size can often vary significantly from the nominal particle size, direct comparison of different gels is often difficult. In addition, post manufacturing handling and/or various derivitization schemes employed prior to column packing may alter the particle size distribution profile. The common proce-

ture of extended ultrasonication during out-gassing is one such procedure which can fracture particles and alter the distribution [3]. Finally, changes in the surface properties of derivitized silicas may alter the aggregation properties of small support particles, and aggregate size analysis may allow comparison of behavior in various solvent systems.

We have investigated the use of time-dependent turbidimetry during the settling of silica gel particles as a means of estimating the size distribution of chromatographic supports. While commercial instrumentation is available for particle sizing, for our purposes this alternative was cost prohibitive, less flexible and does not give the desired information on settling kinetics as a function of solvent. The method exploited here is similar to that suggested by Gumprecht and Sliepcevich [4] but uses a simple spectrometer as a measuring device. Digital data acquisition with a microcomputer was used to manipulate data to yield the various particle size distributions reported.

#### THEORY

The scattering of light by particles which are large relative to the wavelength of the light falls in the realm of Mie scattering. The apparent absorbance (related by the turbidity) of a solution of non-absorbing monodisperse particles in a non-absorbing medium

is proportional to 1) the pathlength ( $b$ ), 2) the concentration of scattering particles of size  $d$  in the light beam ( $C(d)$ ), 3) the square of the particle size ( $d^2$ ), and 4) the scattering coefficient,  $Q$ , which is itself a function of particle size, the wavelength of light used, and the ratio of refractive indices of the particle and the medium ( $m$ ).

$$A = (\text{const})[b C(d) d^2 Q(d, \lambda, m)] \quad (1)$$

Equation 1 is often represented in terms of a dimensionless size parameter,  $\alpha$ , which relates the diameter and the wavelength so that at a given wavelength

$$A = (\text{const})[b C(\alpha) \alpha^2 Q(\alpha, m)] \quad (2)$$

where

$$\alpha = \pi d / \lambda \quad (3)$$

Implicit in the above is the assumption that only transmitted light (i.e., not scattered light) is measured at the detector. In Mie scattering the greatest scattering intensity is directed nearly along the axis of transmission [5] so that proper measurement of exact turbidimetric data requires precise and narrow detector geometries. In practice some scattered light will be measured and the scattering coefficient  $Q$  should be replaced in equation 1 with an effective scattering coefficient  $Q_{\text{eff}}$ , which is also a function of the optical geometry. While formal evaluation of the scattering coefficient involves the solution of Maxwell's

equations, approximate solutions valid at high and low values of  $\alpha$  are more tractable. For silica particles in water, and using 300 nm radiation, the values of the dimensionless size ( $\alpha$ ) are approximately 10 times the particle diameter in microns. Thus for particles above about 2.5 microns the approximate solutions of Van de Hulst and of Walstra [6] can be used to calculate values of the real and effective scattering coefficients as a function of  $\alpha$ , the refractive index ratio, and the angle  $\omega$ , which may be viewed as the finite angle of acceptance of the spectrometer. As shown in Figure 1, the effective scattering coefficient,  $Q_{\text{eff}}$ , rapidly approaches a limiting value of unity as either the particle size (i.e.  $\alpha$ ) or the angle  $\omega$  increases. For simple spectrometers the value of  $\omega$  will be large. In our case the value was estimated to be significantly larger than  $5^\circ$  [6]. The result of this is that to a first approximation, the scattering coefficient term may be taken as a constant independent of particle size, and the absorbance (turbidity) is approximated as being proportional to the square of  $\alpha$ , the concentration, and the path length.

$$A = (\text{constant})[b C(\alpha) \alpha^2] \quad (4)$$

For a polydisperse suspension the total absorbance will then be the integral over all particles of the absorbances of each particle size, or

$$A_{\text{tot}} = \int_0^{\infty} A(\alpha) d\alpha = (\text{constant}) \int_0^{\infty} C(\alpha) \alpha^2 d\alpha \quad (5)$$

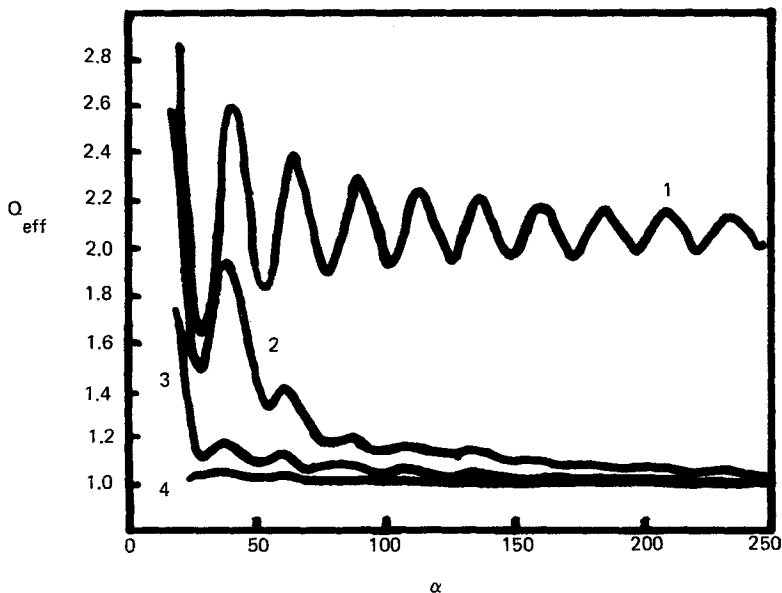


Figure 1. Scattering coefficient ( $Q(\alpha, m)$ ) and the effective scattering coefficient ( $Q_{\text{eff}}(\alpha, m, \omega)$ ) for various values of  $\omega$ . Plots calculated for the approximate forms of Van de Hulst and of Walstra as taken from reference 6. Curves 1-4 denote  $\omega$  values of 0, 2, 5, and 10 degrees, respectively.

A suspension of particles will eventually settle out under the influence of gravity. However, for spherical particles with density greater than that of the suspending medium the particles will settle out at a terminal velocity ( $v(d), \text{cm/s}$ ) given by Stoke's law

$$v(d) = d g (\rho_p - \rho_s) / 18 \eta \quad (6)$$

where  $g$  is the gravitational constant ( $980 \text{ cm/s}^2$ ),  $\rho_p$  the particle's density,  $\rho_s$  the solvent density ( $\text{gm/cm}^3$ ), and  $\eta$  the solvent viscosity (in poise). While Stoke's law is strictly valid only for spherical

particles, it may be used to describe the settling of irregular particles with diameter ratios of up to approximately four with little error [7]. In such cases the so-called Stoke's diameter, or the diameter of a spherical particle with the same volume, is measured. In addition, for porous particles the density of the particle will be decreased relative to that of the solvent due to the inclusion of solvent within the pores of the particle. It is also implicit that the particles are settling in a quiescent liquid and that the particles are large enough that thermal (Brownian) agitation of the particles is negligible.

For an initially homogeneous suspension, as particles of a given size settle from an observation plane (light path) they will be replaced from above by an equal number of particles of the same size until such time as all the particles of that size have settled to a point below the level of the plane. Thus for a defined observation plane at time  $t$  there will be a critical particle diameter given by

$$d_{crit}(t) = [18\eta x / t g(\rho_p - \rho_s)]^{1/2} \quad (7)$$

below which all particle sizes are present at their initial concentrations and above which size the concentration is zero. In the above equation  $x$  is the distance measured from the top level of liquid to the observation plane. Therefore the total concentration



of particles at the observation plane at a given time will be the integral of the initial concentrations of all particles over all particle sizes up to the critical diameter.

Re-expressing equation 7 in terms of dimensionless diameters ( $\alpha$ ) the dependence of the absorbance on time is

$$A(t) = \int_0^{\alpha_{\text{crit}}(t)} A(\alpha) d\alpha = (\text{constant}) \int_0^{\alpha_{\text{crit}}(t)} C(\alpha) \alpha^2 d\alpha \quad (8)$$

which when differentiated with respect to alpha and divided by the square of alpha critical yields

$$C(\alpha) = (dA/d\alpha) / (\alpha^2) \quad (9)$$

This is easily transformed into the size distribution.

#### EXPERIMENTAL

All absorption measurements were made on a Bausch and Lomb Spectronic 88 spectrophotometer. For convenience, the standard cuvette holder was used in place of the universal test tube cuvette holder supplied. No modification of the detector or optics were made in contrast to most true turbidimetry analyses [6] with the exception of masking the cuvette to define the plane of observation. Data was taken at the 2V outputs, digitized, and stored on an Apple II Plus computer (48K) via an ADALAB (Interactive Microware, Inc., State College, PA) ADC. Calculations and data manipulation were carried out via BASIC programs on the Apple computer.

Silica gels analyzed included samples of various batches of LiChrosorb Si60 (Merck, GFR) of 5 and 10 micron nominal particle sizes. Two of these samples were donated by Micromeritics, Inc. (Norcross, GA) and had been analyzed previously with respect to particle size on their Model 5000 SediGraph analyzer. Other samples included LiChrosorb Si60 and Si100 DIOL phases, as well as LiChrosorb Si60 derivatized by various methods with the affinity ligand Cibacron Blue 3G-A. Reverse-phase supports Hypersil ODS 5 micron (Shandon, UK) and Nucleosil 7 C<sub>18</sub> (Macherey-Nagel, GFR) were also studied. Solvents used in this work included doubly deionized water, methanol (Mallinkrodt, HPLC grade), ethanol (University of Minnesota, technical grade), isopropanol (MCB, HPLC grade), toluene (Fisher, scintillation grade), and cyclohexane (Eastman, reagent grade). All solvents were filtered through 0.45 micron filters before use.

The procedure involved weighing out 10-20 (typically 15) mg portions of silica gels and suspending each in 3 ml of solvent. The suspensions of silica gel in solvent were thoroughly outgassed under vacuum with ultrasonication for a short time. To assure disaggregation, samples were also vigorously agitated on a vortex mixer for 1 minute immediately prior to measurement. Timing of the settling commenced with pouring

the suspension into a cuvette which was then placed in the spectrometer. Solvent temperature was recorded at the onset of each experiment and no significant thermal heating of the solution during the settling experiment itself was observed.

In order to define the plane of observation for the scattering, the cuvette was masked off with opaque plastic tape, leaving a 1 mm plane exposed approximately 1 cm from the base of the cuvette. Knowledge of the distance between this plane and the top level of solution in the cuvette is necessary to measure the size distribution ( $x$  in equation 7). Minimum data acquisition intervals varied with solvent and mean size of the silica gel. It was found that 1000 points at a 10 sec. interval yield more than sufficient data density to define the 5  $\mu\text{m}$  support in water. Shorter times can be used for larger particles or solvents with lower viscosities. An example of the typical raw data (absorbance vs. time) is shown in Figure 2. Data acquisition was continued until the absorbance leveled off after a steep decline.

Construction of the size distribution from absorbance-time data was achieved using a BASIC program. Values for the solvent density and viscosity, acquisition time increment, and settling distance ( $x$ ) are required as well as an estimate of the net particle

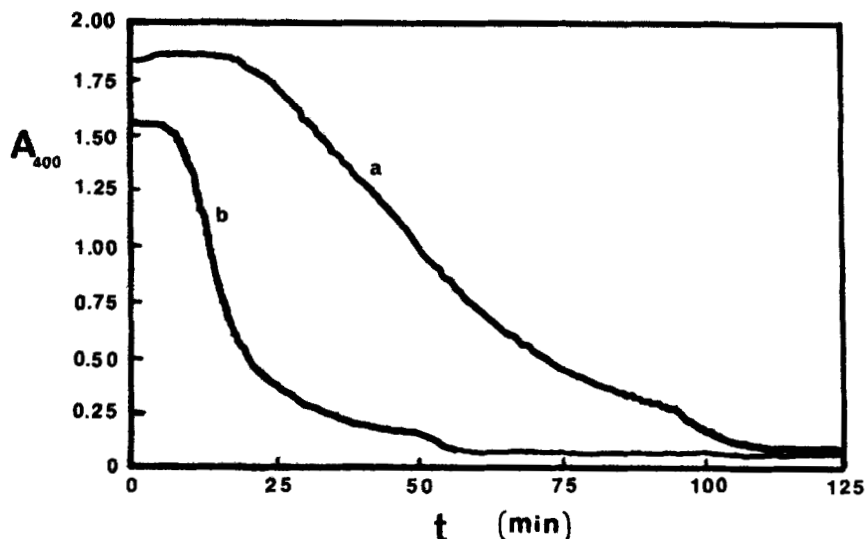


Figure 2. Absorbance-time raw data for a settling experiment. Upper (a) curve shows LiChrosorb Si60 5 micron (nominal size) silica, lower (b) curve is LiChrosorb Si60 10 micron silica. Solvent (both curves) is water, 30°C,  $x=2.00$  cm,  $\lambda=400\text{nm}$ .

density. Values of the density and viscosity for non-aqueous solvents and mixtures at the experimental temperatures were obtained in standard references or were estimated using the procedures in [8]. We have estimated the net particle density by assuming a percent porosity of the particle and calculating a density based on a mean silica density of  $2.36 \text{ gm/cm}^3$  [9] and the percent volumes of the silica and the solvent. Silica densities of  $2.30$  and  $2.46 \text{ gm/cm}^3$  were used for LiChrosorb Si60 and LiChrosphere Si500 supports respectively [9]. Percent porosities for different gels were

estimated on the basis of previous experience with porosities of columns packed with the packing material or on the basis of relative packing densities and pore volumes. In this manner we used a value of  $1.43 \text{ gm/cm}^3$  for the solvated LiChrosorb Si60 particle in water based on a porosity of 67%. It should be noted that the effect of inaccuracies in the estimation of the density is decreased due to the dependence of the particle diameter on the square root of the density. An option to skip over a set number of points was included in the computer program in order to reduce the data density in the differentiation step, if necessary, since high density at low particle sizes increases the scatter in this step.

A 9 point differentiating Savitsky and Golay smooth [10] was used to differentiate the raw data with respect to time. The critical particle sizes and  $\alpha$  values for each time were then calculated and the corrections for differentiation with respect to  $\alpha$  and the  $\alpha$  squared term were performed. The size distributions in terms of number and weight concentrations (arbitrary units) as well as cumulative number and weight distributions versus the critical diameter were automatically computed and plotted on the video screen.

#### RESULTS AND DISCUSSION

Results of the determination of replicate runs of 5 and 10 micron LiChrosorb Si60 supports are shown in

Figures 3 and 4 respectively. In 3a and 4a the number and weight distributions are shown as a function of particle size. The integrated cumulative distributions are shown in the 3b and 4b. Two replicate runs are shown in each case. The open circles in 3b and 4b represent values provided by Merck on the labels for the cumulative weight percent, while the open squares represent the corrected data obtained from the Sedi-graph analyzer. The Sedigraph data was corrected in order to normalize for a different value of the particle density used in the analysis at Micromeritics [11]. The agreement between our cumulative weights with those provided by Merck for these lots is excellent while the agreement of our distributions with those provided by Micromeritics is still quite reasonable. It should be noted that due to the algorithm used in plotting, the areas of different plots have not been conserved.

At very high data densities, for small particles the scatter in the data increases significantly due to the numerical process of differentiation of data evenly spaced in time. As the particles become very small the difference in critical diameters between successive times becomes very small, thereby greatly expanding the scatter due to noise. Time increments of 10 to 100 seconds can be used to cover the range from approximately 3 to 20 micron silica particles. In general we

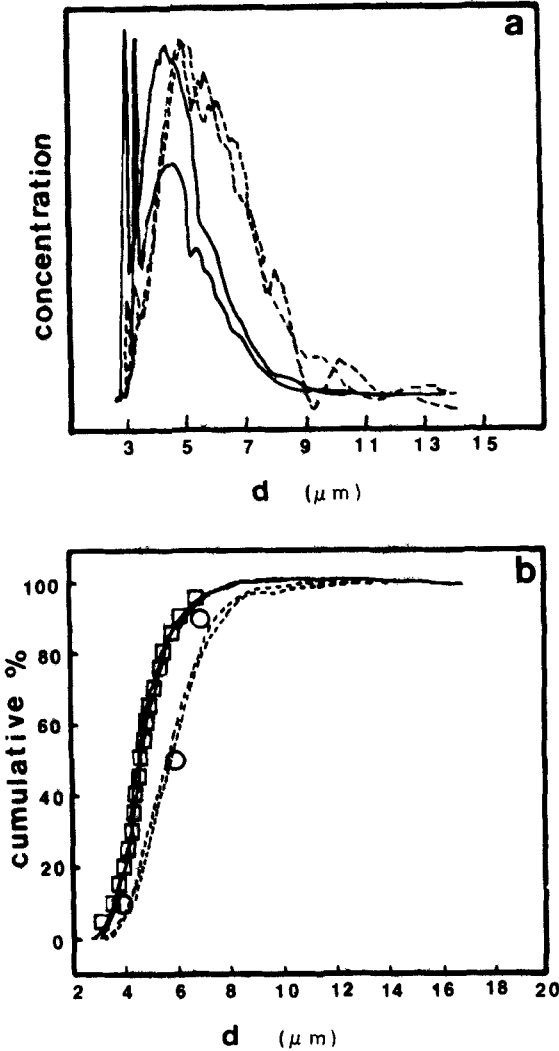


Figure 3. Size distributions for LiChrosorb Si60 silica gel (5 μm). Solid lines depict number distributions while dashed lines depict weight distributions. Replicate runs are shown for each curve. Left plot (a) shows the actual distributions of the data in (a). Squares indicate values obtained by corrected SediGraph analysis while circles indicate Merck provided data.

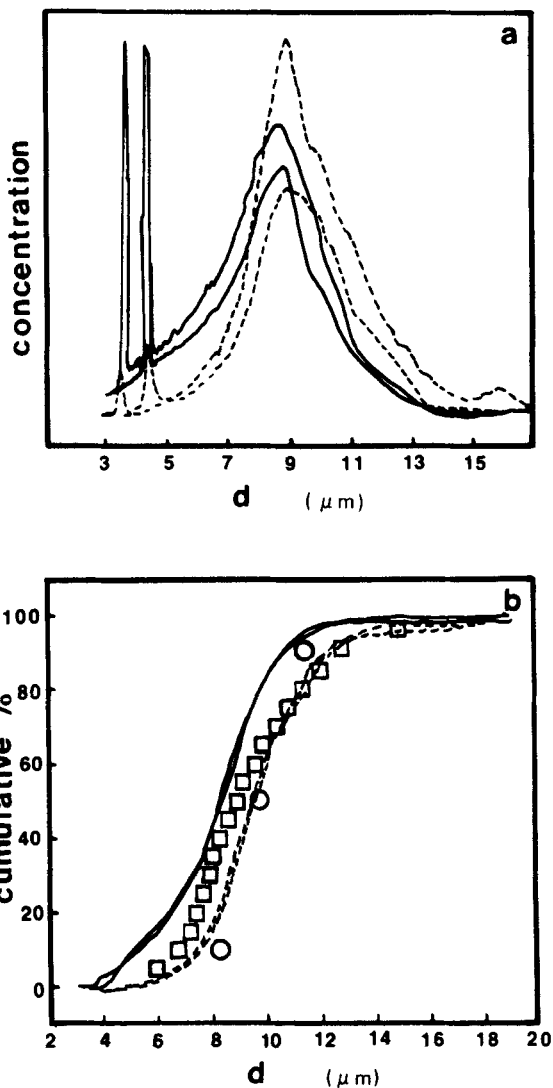


Figure 4. Size distributions for LiChrosorb silica gel (10  $\mu\text{m}$ ). Solid lines depict number distributions while dashed lines depict weight distributions. Replicate runs are shown for each curve. Left plot (a) shows the actual distributions while the right plot (b) shows cumulative distributions of the data in (a). Squares indicate values obtained by corrected Sedigraph analysis while circles indicate Merck provided data.



found 500 points spaced at 20 second intervals provided a reasonable compromise between data density at large diameters and data scatter in the small diameter region. We have obtained reasonable plots using as few as 100 points.

In all the data sets involving underivatized Li-Chrosorb 5 and 10  $\mu\text{m}$  particles a significant change in the absorbance curve occurred at times corresponding to silica particles of approximately 3 and 4 microns respectively. We are uncertain of the origin of this phenomenon which manifests itself as the brief region of a high concentration (highly scattered) of particles at the very lower extreme of the distribution. Identical results were obtained at both 400 and 800 nm, indicating that this is not an anomaly of the particular scattering conditions. We speculate the existence of fine particles of much higher density for which the settling rate is the same as that for approximately 4  $\mu\text{m}$  support particles. The algorithm would interpret these co-settling fine particles as a higher concentration of the larger support particles. In such a case, the high scatter in this region on the distribution plots would not signify an actual deviation in the shape of the tail of the distribution of the support particles. In any case the total effect on the cumulative number distribution is small and is negligible on

the cumulative weight distribution. This phenomenon was not observed with the same LiChrosorb gels after treatment to derivitize the particles with a DIOL functionality. In addition, the similarity of results at 400 and 800 nm wavelengths is strong support of our assumption that the effective scattering coefficient is virtually independent of  $\alpha$  for our spectrometer, since changing the wavelength will alter the  $\alpha$  value (see eqn. 3). If the scattering coefficient was changing significantly with  $\alpha$  the greatest differences between 400 and 800 nm experiments should be noted at small particle sizes where our agreement is still good.

While the settling time for very small particles can be quite long, use of a solvent with lower density and/or viscosity will decrease the required time. In this case, however, changes in the surface wetting characteristics due to variation in other physical properties, e.g. the surface tension, may alter particle agglomeration properties and change the distribution. We examined LiChrosorb DIOL supports in various solvent systems and found that the DIOL settling behavior in water, methanol, and ethanol varied systematically and quantitatively as expected from equation 6 with changes in solvent density and viscosity. For these solvents the cumulative weight average particle sizes ( $d_{50}$ ) were calculated to be between 10.7 and 11.8

microns. Drastically different behavior was observed in isopropanol, toluene, and cyclohexane, which can be attributed to particle agglomeration in these solvents. The values for the measured apparent  $d_{50}$  values in these solvents were 13.8, 23.1, and 29.0 microns, respectively. The distributions of the particles in methanol, isopropanol, toluene, and cyclohexane are shown in Figure 5. Similar results were observed for both commercial and in house preparations of the DIOL phase. The shift in the measured distribution to particles of larger (apparent) size also suggests that particle agglomeration is occurring. The actual size of the larger particles may not be accurately reflected by the abscissa value as the agglomerate net density probably varies from the assumed value for single particles due to a probable change in the effective porosity of the agglomerate. Because the algorithm assumes a single density value for all particles, increased porosity in agglomerates, due to the interparticle volume, would actually result in a larger particle size than shown.

The data from the DIOL phases agrees well with the expected results based upon the assumption that highly polar particles will agglomerate in very non-polar solvent to minimize the exposed surface area. The results in isopropanol are nonetheless surprising. The solvent order in which agglomeration apparently occurs

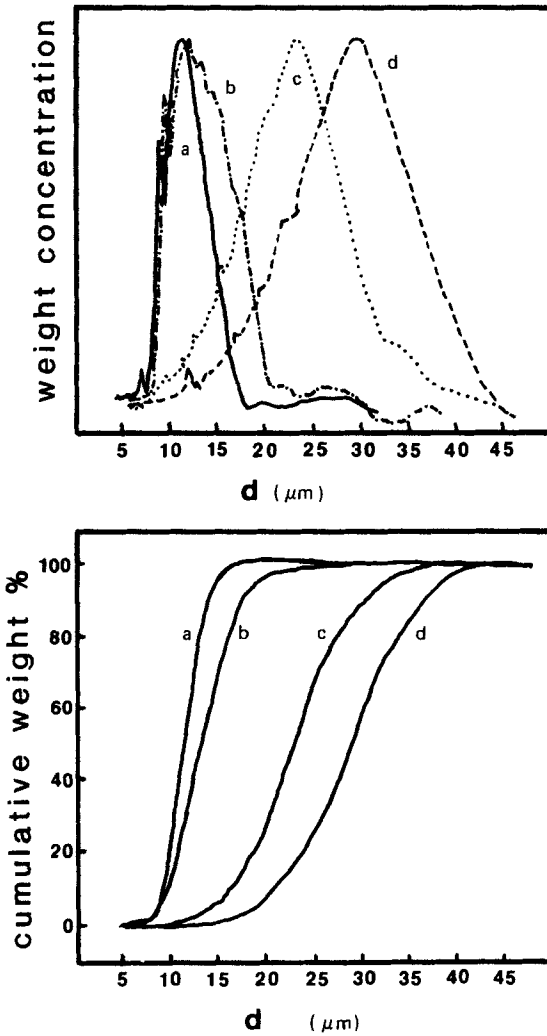


Figure 5. Particle weight distributions of LiChrosorb Si60 DIOL (10 m) samples in the solvents (a) methanol, (b) isopropanol, (c) and toluene, and (d) cyclohexane. The cumulative weight distributions are shown in the lower plot.

is consistent with the solvent polarity as measured by Snyder's polarity (P') scale [12] in which the order of solvents decreases in the sequence as water > methanol > ethanol > isopropanol > toluene > cyclohexane.

Less solvent dependent results were obtained using the reverse-phase octadecylsilyl derivitized support Hypersil ODS (5 $\mu$ m) in various non-aqueous solvents. Results for Hypersil in methanol, ethanol, isopropanol, toluene, and cyclohexane indicate no significant agglomeration occurs for the reverse-phase support in these solvents. Weight distributions for the Hypersil ODS in methanol, isopropanol, and cyclohexane shown in Figure 6 illustrate this point. The dry silica density of 2.36 gm/cm<sup>3</sup> and a net porosity of 45% was used in calculations for this material. Water was not tested due to its inability to wet the support, so in order to test the effect of increased solvent polarity on the settling behavior of the Hypersil ODS supports, an electrolyte was added to methanol. The use of 12 millimolar hydrochloric acid in methanol as solvent resulted in doubling the average particle size relative to the value in pure methanol. When the solvent was comprised of 16 millimolar ammonium hydroxide, however, a slight decrease in the average particle size relative to pure methanol was noted. These results can be understood both in terms of agglomera-

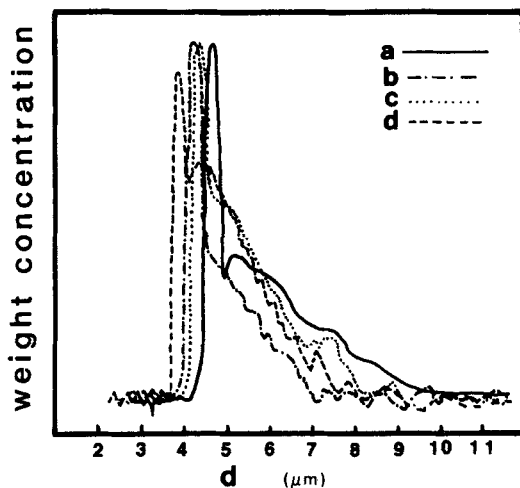


Figure 6. Particle weight distributions of Hypersil (5  $\mu\text{m}$ ) ODS samples in the solvents (a) methanol, (b) isopropanol, (c) toluene, and (d) cyclohexane.

tion of a non-polar support in the polar solvent and in terms of the existence of an electrostatic barrier to agglomeration created by residual surface charge. In the former case the addition of hydrochloric acid to the solvent should result in a decrease of the net surface charge due to the increased degree of protonation of residual surface silanols, thereby reducing the electrostatic barrier to agglomeration. In the case of added ammonia, the degree of silanol ionization should increase, creating a net negative charge on the particle [1] for which the electrostatic repulsion opposes agglomeration and offsets the effect of the increased solvent polarity.

A strong solvent dependence of the settling behavior was also observed for DIOL phases derivitized with the triazine dye Cibacron Blue 3G-A. Figure 7 shows size distributions for LiChrosphere Si500 DIOL, derivitized with Cibacron Blue by the procedures of Mosbach et al. [13], in various solvents. The anionic triazinyl dye is a polysulfonated aromatic ring system covalently bound to the DIOL phase via a 1,6-hexane diamine spacer arm at very low surface concentrations (ca. 10 nmole/m<sup>2</sup>). While the equations derived earlier do not strictly hold in the case in absorbing scatterers (Cibacron Blue absorbs somewhat throughout the visible spectrum) the above approach should be able to differentiate changes in the shape of the size distribution between solvents. This is seen in Figure 7 in which the differences in the size distributions in methanol, isopropanol, toluene, and cyclohexane again suggest that agglomeration is occurring. In comparison with their precursor DIOL phases, the Cibacron modified phases display a similar pattern but appear to be slightly more hydrophilic, which is consistent with the existence of several highly polar and ionic functional groups on the dye molecule. While a detailed knowledge of the interactions between solvent and Cibacron supports is unknown at this time the data suggests that at least the non-polar solvents interact with the

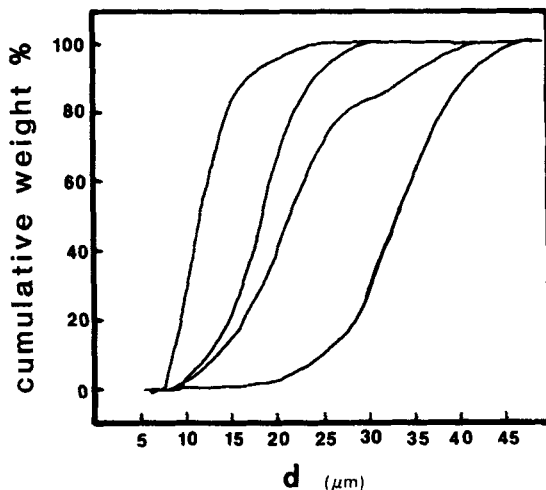


Figure 7. Cumulative weight distributions of samples of Cibacron Blue 3G-A modified LiChrosphere S1500 DIOL in the solvents (a) methanol, (b) isopropanol, toluene, and (d) cyclohexane.

support in a very different manner than do polar solvents.

Figure 8 summarizes the results of experiments on five different silica supports in various solvent systems. The abscissa in Figure 8 represents the measured value of the cumulative weight average particle size ( $d_{50}$ ) for the given silica gel in the specified solvent system. Silica gel 1 is the underivitized 5 and 10 micron LiChrosorb Si60 while silica 2 is the data from the 5 micron Hypersil ODS support. Silica 3 is LiChrosorb Si60 DIOL and silicas 4 and 5 are Cibacron modified phases. Silica 4 is lightly loaded with



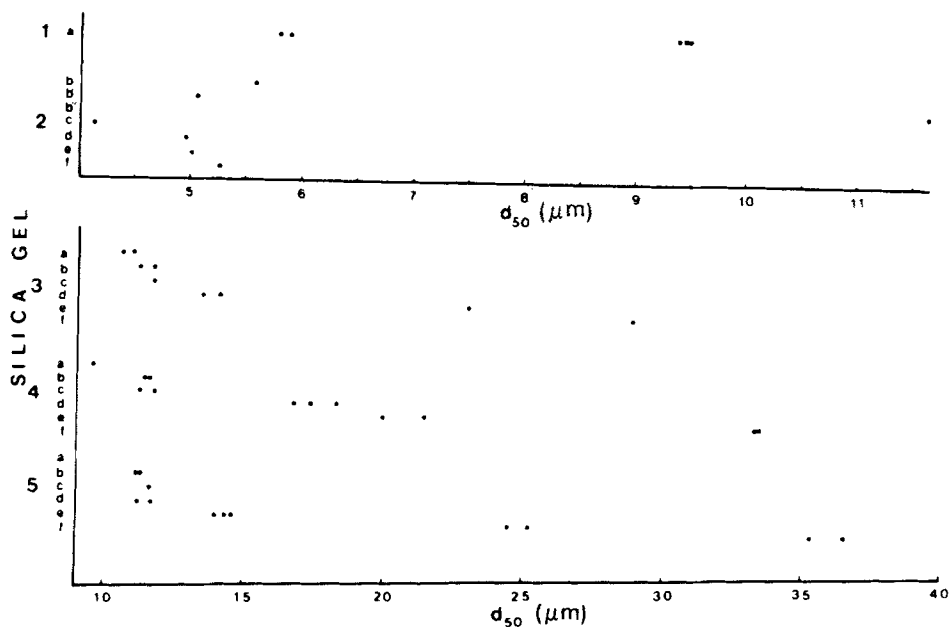


Figure 8. Summary of the dependence of the observed 50% cumulative weight diameter ( $d_{50}$ ) on the solvent for a variety of silica gels: (1) underivitized LiChrosorb Si60 5 and 10  $\mu\text{m}$  particles, (2) Hypersil (5  $\mu\text{m}$ ) ODS, (3) LiChrosorb Si60 DIOL, (4) Cibacron modified (Mosbach prep) LiChrosphere Si500 DIOL and (5) Cibacron modified (directly coupled) LiChrosorb Si60 DIOL. Solvents are designated as (a) water (b) methanol, (b') 16 nM  $\text{NH}_4\text{OH}$  in methanol, (b'') 12 nM HCL in methol, (c) ethanol, (d) isopropanol, (e) toluene, and (f) cyclohexane.

ligand immobilized via the hexanediamine spacer arm as described above, while silica 5 is a much heavier loading of directly bonded (no spacer arm) dye. The solvent symbols are given in the figure legend.

#### CONCLUSIONS

The results obtained by this method of studying the particle size distribution are comparable to those

of other methods for silica chromatographic supports. Because the method fundamentally estimates the number distribution most other widely used definitions of the distribution can be readily calculated. The method uses only common laboratory experiment. The parameters necessary involve an estimation of the density of the particles in the solvent, a measurement of the settling distance, and values of the solvent density and viscosity. Of these the particle density can be obtained based on an approximation of the porosity of the particle. In addition to determination of the size distribution for the purposes of column efficiencies, the method can be useful in the evaluation of solvent effects on particle agglomeration. By evaluating the size distribution of a support matrix in various solvent systems and comparing the results, significant information can be inferred as to the nature of the particle surface and solvent wetting under the experimental conditions. By means of an example, settling rates and size distribution data for Cibacron Blue affinity chromatographic supports suggest substantial particle agglomeration occurs in non-polar solvents, implying a strongly polar character to the surface. Knowledge of the particle settling rates and agglomeration properties can be useful in the optimization of solvent conditions during column packing.

ACKNOWLEDGEMENTS

Work in this paper has been funded in part by grants from the Minnesota Mining and Manufacturing Co., St. Paul, MN, and from the National Science Foundation (CHE 8217363).

REFERENCES

1. Snyder, L.R. and Kirkland, J.J., Introduction to Modern Liquid Chromatography, 2nd ed., John Wiley and Sons, NY, 1979.
2. Bristow, P.A., J. Chromatogr., 149, 13-28 (1978).
3. Halasz, I. and Ohmacht, R., Chromatographia, 14(3), 155-162 (1981).
4. Gumprecht, R.O. and Sliepcevich, C.M., J. Phys. Chem., 57, 95-97 (1953).
5. Billmeyer, F.W., "Principles of Light Scattering" and Hochgesang, F.P., "Nephelometry and Turbidimetry" in Treatise on Analytical Chemistry, Part I, Vol. 5, Kolthoff, I.M. and Elving, P.J, (eds.), John Wiley and Sons, pp. 2839-2872 and 3289-3328 , 1964.
6. Melik, D.H. and Fogler, H.S., J. Coll. Int. Sci., 92, 161-178 (1983).
7. Cadle, R.D., Particle Size, Theory and Industrial Applications, Reinhold Publishing Corp., NY, pp. 82-4, 1965.
8. Reid, R.C., Prausnitz, J.M., and Sherwood, T.K., The Properties of Gases and Liquids, 3rd ed., McGraw-Hill, NY, 1977.
9. Unger, K.K., Porous Silica: Its Properties and Its Use as a Support in Liquid Chromatography, Elsevier, Amsterdam, 1979.
10. Savitsky, A. and Golay, M.J.E., Anal. Chem., 36(8), 1627-38 (1964).
11. Rootare, H.M., Correcting Sedigraph Curves for Samples Run with Incorrect Rate, Micromeritics, Inc., Norcross, GA.

12. Snyder, L.R., J. Chromatogr. Sci., 16, 223-231 (1978).
13. Lowe, C.R., Glad, M., Larsson, P., Ohlson, S., Small, D., Atkinson, T., and Mosbach, K., J. Chromatogr., 215, 303-316 (1981).